

EVOLUTIONARY RELATIONSHIPS OF *MYCAUREOLA DILSEAE* (AGARICALES), A BASIDIOMYCETE PATHOGEN OF A SUBTIDAL RHODOPHYTE¹

MANFRED BINDER,^{2,4} DAVID S. HIBBETT,² ZHENG WANG,² AND WILLIAM F. FARNHAM³

²Biology Department, Clark University, Lasry Science Center, 950 Main Street, Worcester, Massachusetts 01610-1477 USA; and

³Institute of Marine Sciences, University of Portsmouth, Eastney, Portsmouth, Hants, PO4 9LY, UK

Mushroom-forming fungi (homobasidiomycetes) are major examples of morphological and ecological diversification in terrestrial habitats. Homobasidiomycetes includes only nine described species that are known from marine environments. Morphological traits that have concealed the ancestry of these fungi include reduced fruiting bodies with hairy surfaces and extremely modified spores, both of which may function as floating devices to aid successful dispersal and adhesion to various substrates such as driftwood. Our previous results suggested that all marine forms as yet investigated are placed in the *Nia* clade (euagarics) and that they have primarily evolved from cyphelloid forms (minute, cup-shaped, terrestrial saprotrophs) via transitions through mangroves to fully marine habitats. We show here that *Mycaureola dilseae*, which parasitizes the red alga *Dilsea carnosa*, is a second independent lineage of marine fungi in the euagarics clade that is not related to cyphelloid forms. Phylogenetic reconstructions were based on two data sets: a partial four-region rDNA data set (nuc-ssu, nuc-lsu, mt-ssu, and mt-lsu) with inclusive sampling of 249 taxa and a densely sampled ITS data set including 32 taxa, which formed a clade with *Mycaureola* in the four-region rDNA analyses. Inferences using constrained and unconstrained six-parameter weighted parsimony, Bayesian Markov chain Monte Carlo methods, and maximum likelihood approaches place *M. dilseae* in the morphologically diverse /phylaciaceae clade next to *Gloiocephala* spp., a group of highly reduced stipitate-pileate saprotrophs.

Key words: cyphelloid fungi; euagarics clade; marine homobasidiomycetes; morphological reduction; multilocus rDNA analyses.

Homobasidiomycetes (phylum Basidiomycota), or the mushroom-forming fungi, have radiated extensively in terrestrial habitats and have occupied any ecological niche conceivable. The morphological diversity in this group is complex and frequently the result of evolutionary parallelisms and reversals (Hibbett et al., 1997; Hibbett and Binder, 2002; Hibbett, 2004). Typical fruiting body plans of homobasidiomycetes include stipitate-pileate forms (mushroom-like, a stalk bearing the cap), resupinate (crust-like) forms, coral fungi, gasteroid fungi (false truffles with the spore-bearing layer enclosed), and other sessile forms. Only a few homobasidiomycetes have adapted secondarily to marine environments, in many cases undergoing morphological transformations and reductions that make it difficult to identify their closest terrestrial relatives. Six genera including nine species are known from marine habitats (Kohlmeyer and Kohlmeyer, 1979; Hyde et al., 2000).

The subject of this study is the phylogenetic placement of *Mycaureola dilseae* (Maire and Chemin) emend. Porter and Farnham, a monotypic marine pathogen of the red alga *Dilsea carnosa* (Schmidel) Kuntze (Dumontiaceae). *Mycaureola dilseae* was originally published as a pyrenomycete (phylum Ascomycota) because it distinctly resembles bottle-shaped fruiting bodies that are characteristic for this group of ascomycetes (Maire and Chemin, 1922). Porter and Farnham (1986) using TEM techniques showed that the hyphae of *M.*

dilseae have dolipore septa with perforate parenthesomes, which places the fungus in the basidiomycetes. Their report is the only one on a basidiomycete parasitizing a rhodophyte (or any other group of macroalgae), and there are few clues, if any, about potential terrestrial relatives. *Mycaureola* is host-specific and its distribution is therefore limited to the northern temperate area of *D. carnosa* ranging from Russia to Portugal. Mature fruiting bodies of *M. dilseae* are white, hemispherical with an apical opening (ostiolum) measuring 0.3–0.5 mm, and it produces unproportionally large sigmoid spores (105–118 µm), which are among the largest in the basidiomycetes (Fig. 1; Porter and Farnham, 1986). It has been assumed that the spores are passively discharged (statismosporic); however, the mechanisms behind spore discharge under water and spore transmission to healthy populations of *D. carnosa* are unknown. Infection seems to be directed primarily at algal blades (Chemin, 1921) and progresses in several stages (Fig. 2), which were described in detail by Porter and Farnham (1986). *Nia vibrissa* R. T. Moore and Meyers, one of the known marine homobasidiomycetes that resembles *M. dilseae* fruiting bodies most, uses statismosporic spore dispersal, but *N. vibrissa* fruiting bodies remain unopened (gasteroid), and the spores have appendages and a tetra- or poly-radial shape (Moore and Meyers, 1959).

Recent phylogenetic studies have shown that all four marine genera reported previously were in the euagarics clade (Binder et al., 2001; Hibbett and Binder, 2001), which is the most species-rich clade of homobasidiomycetes including approximately 9400 described species (Kirk et al., 2001). Three marine forms, *N. vibrissa*, *Halocyphina villosa* Kohlm., and *Calathella mangrovei* E. B. G. Jones and Agerer, were strongly supported to form a monophyletic group nested within several terrestrial, cyphelloid fungi (bootstrap = 100%), the so-called *Nia* clade (Hibbett and Binder, 2001). Cyphelloid basidiocarps are

¹ Manuscript received 31 August 2005; revision accepted 24 January 2006.

This study was supported by NSF grant DEB-0128925 to D.S.H. and M.B. The authors thank D. E. Desjardin, E. Horak, K. Hughes, P. Inderbitzin, E. B. Gareth Jones, and R. Petersen for providing specimens and comments, and R. Henrik Nilsson for writing and updating the Bayesparser Pearl script. D. Porter and D. L. Hawksworth (on behalf of the British Mycological Society) granted permission to republish Fig. 1.

⁴ Author for correspondence (e-mail: mbinder@clarku.edu)

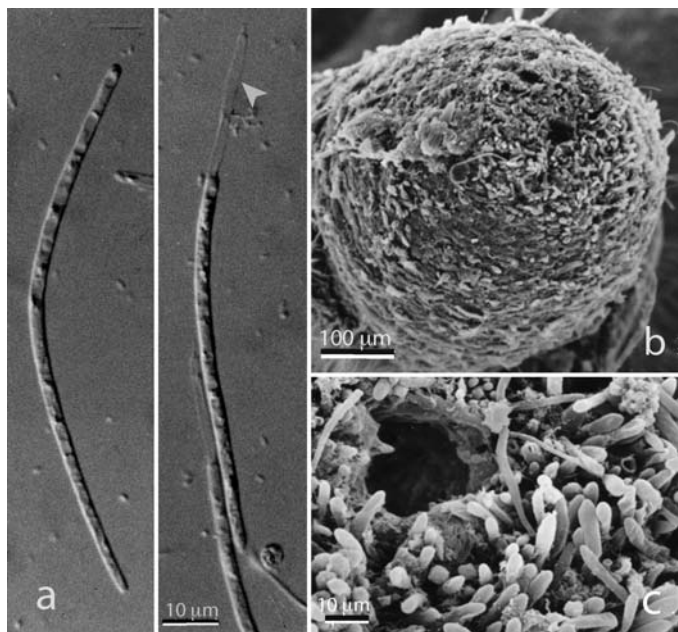


Fig. 1. SEM micrographs of basidiospores and basidiocarps of *Mycaureola dilseae*. (a) one-celled sigmoid basidiospores, with occasional cytoplasm-free partitions (arrowhead); (b) hemispherical fruiting body, apical view; (c) magnification of ostiolar area and surrounding hyphal hairs in (b).

cupulate or tubular in shape and rarely exceed 2 mm in size. The outer surface is usually covered by hairlike hyphae, which may be branched or incrustate, while the hymenium (spore producing layer) covers the interior and is protected within the central concavity. These fungi have at least 10–12 independent origins in the euagarics clade and are presumably derived from stipitate-pileate agaricoid ancestors via morphological reduction (Bodensteiner et al., 2004).

The fourth marine basidiomycete investigated is *Physalacria maipoensis* Inderbitzin and Desjardin, which was placed outside the Nia clade in the study of Hibbett and Binder (2001) as the sister group of the cyphelloid species *Henningsomyces candidus* (Pers.) O. Kuntze. The lack of support for this relationship was probably affected by the limited taxon sampling in their study using four rDNA genes (nuclear and mitochondrial small and large subunits) for 46 representative species of basidiomycetes. In addition, *Physalacria* Peck species differ from a cyphelloid habitus by producing minute, stipitate-capitate (inflated, headlike caps) basidiocarps. A more inclusive study by Moncalvo et al. (2002), who used 877 nuclear large subunit sequences of euagarics placed *Physalacria* aff. *oriconensis* Pat. and Gaillard in a clade they called the /physalacriaceae clade, which is composed of a morphologically diverse group of widely distributed, white rotting fungi. If the placement of *P. maipoensis* is consistent with the results of Moncalvo et al. (2002), then this would suggest that the /physalacriaceae clade contains a second independent lineage of marine homobasidiomycetes in the euagarics.

The objectives of this study were (1) to assemble a partial four rDNA region (nuc-ssu, nuc-lsu, mt-ssu, mt-lsu) data set and to increase taxon sampling with available nuc-lsu sequences of representative species in the euagarics clade

guided by BLAST searches to find a placement for *M. dilseae* using maximum parsimony and Bayesian approaches, (2) to test the hypothesis of multiple origins of marine fungi in the euagarics clade using constrained analyses, (3) to generate ITS data for a subset of species based on the results of (1) that are potentially related to *M. dilseae* and to use maximum likelihood analyses to identify its closest terrestrial relatives, and (4) to design *M. dilseae* specific ITS primers and survey infected and uninfected algal tissues using PCR, which may provide evidence that *M. dilseae* is distributed within the algal population by spore dispersal.

MATERIALS AND METHODS

Taxon sampling and molecular data sets—Fifty-two sequences from 23 species that are potentially related to *M. dilseae* were newly generated and included nuclear and mitochondrial small and large subunit ribosomal DNA (nuc-ssu, nuc-lsu, mt-ssu, mt-lsu, respectively) and the internal transcribed spacer (ITS) region. The sequences have been deposited at GenBank (Appendix).

Two data sets were assembled for this study, a partial four-region rDNA (nuc-ssu, nuc-lsu, mt-ssu, mt-lsu) data set, which was expanded by nuc-lsu sequences and an exhaustive ITS data set. One hundred and seventy-seven taxa were selected based on the studies of Hibbett and Binder (2001, 2002) and Bodensteiner et al. (2004) to represent the major lineages of cyphelloid and aquatic fungi, reduced forms, and their closest relatives in the euagarics clade. Seventy-two nuc-lsu sequences drawn from the study by Moncalvo et al. (2002) were selected to represent stipitate-pileate (agaricoid) forms in the data set. The partial four-region rDNA data set included 249 taxa, which were all represented by a nuc-lsu sequence. Additional data (62 nuc-ssu sequences, 55 mt-ssu sequences, and 41 mt-lsu sequences) were available for some taxa. The goal of this multigenic approach was to identify a focal clade including *M. dilseae* and to select a subset of taxa limited to the focal clade, which allows the use of ITS sequences to address questions about the closest relatives of *M. dilseae* on a fine-scale level.

DNA extraction, PCR, cloning, sequencing, and sequence alignment—Herbarium specimens and cultures provided adequate amounts of material and DNA was extracted by using a phenol–chloroform extraction protocol (Lee and Taylor, 1990). Genomic DNA from minute samples of single fruiting bodies <0.3 mm (e.g., some *Gloiocephala* spp., *M. dilseae*) was isolated using the E.Z.N.A. Forensic DNA kit (Omega Bio-Tek, Doraville, Georgia, USA), which is designed to extract DNA from marginal source material. Fruiting bodies of *M. dilseae* that are infrequently found on the inner edges of advanced lesions were isolated from revived algal tissue using sterile microscalpels. Approximately 50 samples of algal tissue from necrotic lesions lacking *M. dilseae* basidiocarps and from uninfected areas were taken and cut into 2 × 2 mm wide blocks, and stored in a –20°C freezer. The frozen tissue was then ground using micropestles and digested in 0.1 µg/µL lyticase (Sigma, St. Louis, Missouri, USA) for 30 min at room temperature to solubilize intercellular hyphae of *M. dilseae*. The cell lysates and fruiting body isolates were processed using the E.Z.N.A. Forensic DNA kit without additional modifications.

DNA was diluted up to 100-fold with deionized water for use as a PCR template. PCR reactions were performed for three nuclear and two mitochondrial rDNA regions using the primer combinations ITS1-F-ITS4 (ITS region including the 5.8S gene), LR0R-LR5 (nuc-lsu), PNS1-NS41 and NS19b-NS8 (nuc-ssu), ML5-ML6 (mt-lsu), and MS1-MS2 (mt-ssu). Sequences of the primers used in this study have been described elsewhere (Vilgalys and Hester, 1990; White et al., 1990; Hibbett, 1996; Moncalvo et al., 2000). The amplifications were run in 35 cycles on a PTC-200 thermal cycler (MJ Research, Waltham, Massachusetts, USA) using the following parameters: denaturation 94°C (1 min), annealing 50°C (45 s), extension 72°C (1.5 min). PCR products were purified with Pellet Paint (Novagen, EMB Biosciences, San Diego, California, USA). The *M. dilseae*-specific ITS primers, which are nested within the ITS1-F-ITS4 product, were designed based on a preliminary ITS sequence obtained from a fruiting body to detect the phycoparasite in asymptomatic tissue samples. The sequences are (5'-3') CAT TAT TGA AAT TTA TTT TCA (MDITS1, forward) and AAC CAT TAT ATA AAA GTT ACT (MDITS2, reverse).

In addition, two ITS1-F-ITS4 products of *M. dilseae* were cloned using

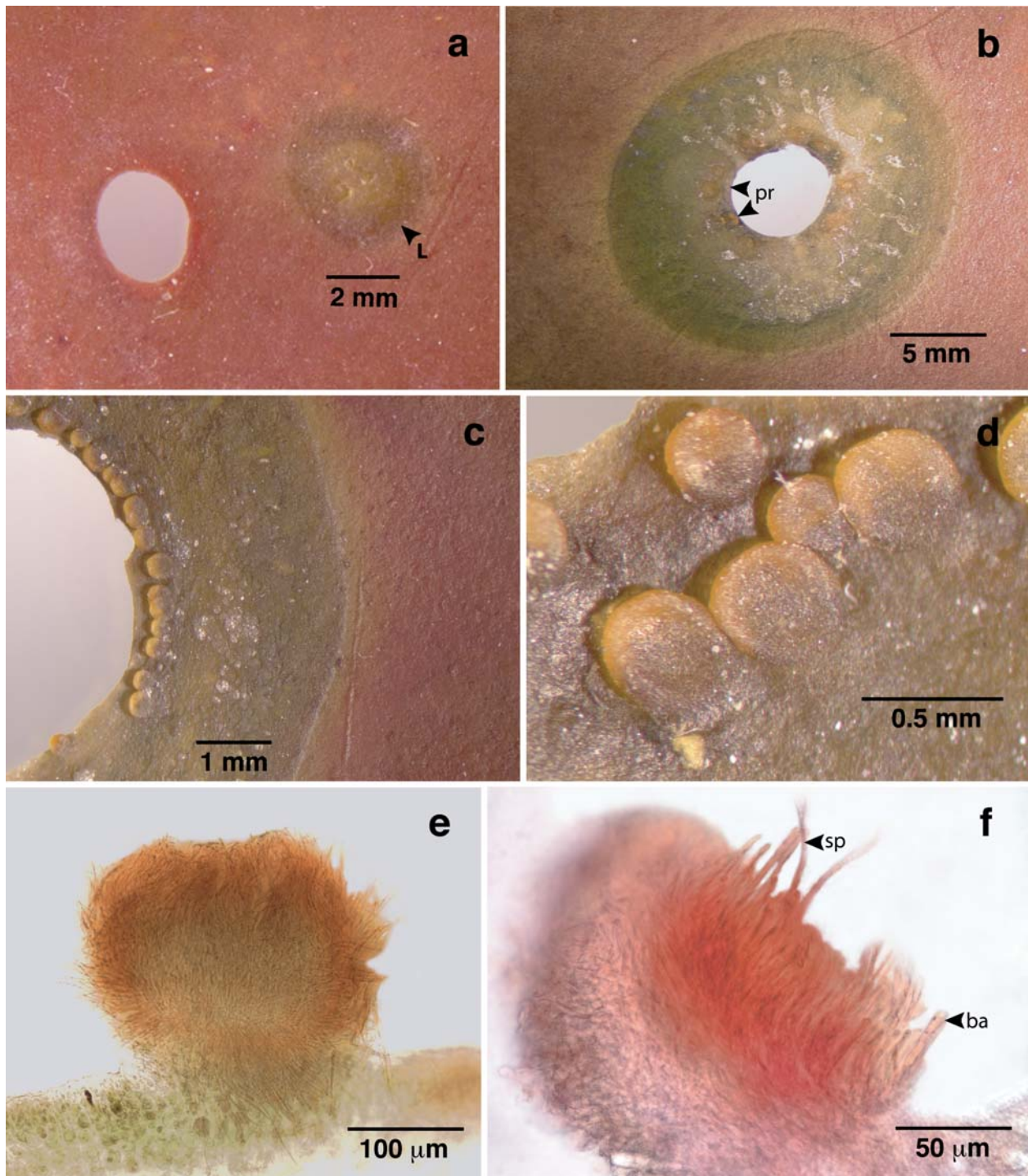


Fig. 2. Photographs (a–d) showing the succession of the disease caused by *M. dilseae* on a blade of *Dilsea carnosa*. (a) formation of a necrotic lesion (L) indicated by phycobilin breakdown; (b) The center of the lesion is degraded, leaving a shot hole appearance to the blade, during the extended nutritional phase: first primordia (pr) appear around both sides of the edges. (c) Fruiting bodies form in clusters and (d) become fully developed. (e) Light micrograph of tangential section through a fruiting body of *M. dilseae* in algal tissue. Hyphae stained with congo red. (f) Light micrograph of cross-section through a fruiting body showing basidia (ba) and developing spores (sp). Hymenium selectively stained with congo red. Micrographs a–d of herbarium material were taken with a Nikon SMZ800 dissecting microscope and a Spot RT slider digital camera (Diagnostic Instruments, Sterling Heights, Michigan, USA), and e–f of rehydrated herbarium material were taken with a Nikon Eclipse E600 microscope and a Spot RT slider camera.

TOPO TA cloning (Invitrogen, Carlsbad, California, USA) to scrutinize for algal byproducts and to detect potentially present epiphytes, which are prevalent on *D. carmosa* blades and may include marine ascomycetes. Cleaned PCR products were inserted into the pCR 2.1-TOPO vector and transformed using the One Shot competent cell kit (Invitrogen). The cells were plated and incubated overnight on LB medium containing 50 µg/mL kanamycin, which was saturated with 50 µL X-gal (Matheny, 2004). Five positive transformants each were directly analyzed with PCR using M13 forward (-20) and M13 reverse primers.

All PCR products were sequenced using BigDye terminator sequencing chemistry (Applied Biosystems, Foster City, California, USA), purified with Pellet Paint, and run on an Applied Biosystems 377XL automated DNA sequencer. Contiguous sequences were assembled and edited using Sequencher 4.1 (GeneCodes Corp., Ann Arbor, Michigan, USA). Automated alignments obtained by using ClustalX (Thompson et al., 1997) were manually adjusted in MacClade 4.0 (Maddison and Maddison, 2000). The alignment of the ITS data set was constrained by secondary structure elements (paired regions or helices), which were inferred from selected species analyzing ITS1 and ITS2 spacer regions separately with mFOLD (Zuker et al., 1999).

Phylogenetic analyses of the partial four-region rDNA data set—Tests for congruence using bootstrap criteria—To investigate potential conflicts among different rDNA genes, a preliminary series of parsimony bootstrap analyses was performed in PAUP* version 4.0b10 (Swofford, 2002), estimating gene phylogenies separately from complete four-region data. Nuclear rDNA genes (nuc-rDNA) of 62 species were combined into a single partition; mt-ssu rDNA of 55 species and mt-lsu rDNA of 41 species were analyzed as individual partitions as well as in combined mode (mt-rDNA). Each bootstrap analysis was performed using 1000 replicates, all characters equally weighted, one random taxon addition sequence, tree-bisection-reconnection (TBR) branch swapping, with MAXTREES set to 10 000. Incongruence among data partitions was evaluated by setting a threshold of bootstrap values >90% to identify positively conflicting nodes (de Queiroz, 1993). A final bootstrap analysis using 300 replicates with the settings just described was performed on the combined four-region data set, which was then extended by 187 nuc-lsu sequences to its final size of 249 taxa.

Six-parameter weighted parsimony—Differentially weighted parsimony was used to compensate for nucleotide substitution rate biases between nuc- and mt-rDNA partitions. Constrained and unconstrained parsimony ratchet (PR; Nixon, 1999) analyses were performed under a six-parameter weighting regime (Williams and Fitch, 1990), which obtains weights for parsimony analyses based on rates of nucleotide substitutions estimated with maximum likelihood (Cunningham, 1997; Stanger-Hall and Cunningham, 1998). Nucleotide transformation rates were estimated in PAUP* under the general time reversible (GTR) model, with equal rates of evolution for all sites and empirical base frequencies, using a tree and data matrix from Binder and Hibbett (2002) that includes 93 species, each with nuc-ssu, nuc-lsu, mt-ssu, and mt-lsu rDNA. Rate matrices for nuc-rDNA and mt-rDNA were converted separately into step-matrices of transformation costs. For nuc-rDNA, the step-matrix values were A-C = 3, A-G = 2, A-T = 2, C-G = 2, CT = 1, GT = 3; for mt-rDNA, the step-matrix values were A-C = 2, A-G = 1, A-T = 2, C-G = 3, CT = 1, GT = 2. Six-parameter weighted PR analyses were performed with PAUP* and PAUPRat (Sikes and Lewis, 2001), using 20 runs in batch mode including 200 iterations each, with 15% of the characters reweighted in each iteration. The analysis was rerun under a topological constraint (the marine basidiomycetes *Halocyphina villosa*, *Mycaureola dilseae*, and *Nia vibrissa* were forced to form a clade, leaving the remaining topology of the tree unresolved) to evaluate the hypothesis of independent origins of marine forms in the euagarics clade. Constrained and unconstrained trees were evaluated with the KH test (Kishino and Hasegawa, 1989) and the SH test (Shimodaira and Hasegawa, 1999).

Bayesian analyses applying heterogenous models—The GTR model (Yang, 1994) using proportion of invariant sites and distribution of rates at variable sites modeled on a discrete gamma distribution with four rate classes was estimated with MODELTEST version 3.06 (Posada and Crandall, 2001) as best-fit likelihood model for both nuclear and mitochondrial partitions; however, model parameters varied considerably. Bayesian analyses on the combined data set were therefore implemented estimating optimal model parameterization for both partitions separately. The GTR model was specified as prior for both nuc- and mt-rDNA partitions, assuming equal probability for

all trees and unconstrained branch length. The substitution rate matrix, transition–transversion rate ratio, character state frequencies, gamma shape parameter α , and proportion of invariant sites were unlinked across nuclear and mitochondrial partitions and calculated independently by MrBayes v3.0b4 (Ronquist and Huelsenbeck, 2003). A user-defined tree (the tree with the highest likelihood, $-\ln L = 48717.306$, found in a test run on the concatenated data set employing 1×10^6 generations) served as a starting tree for all Bayesian analyses. Posterior probabilities for the Bayesian approach were determined twice by running one cold and three incrementally heated Metropolis-coupled Markov chain Monte Carlo (MCMC) analyses for 3×10^6 generations, saving trees every 100th generation. The final burn-in period of trees cumulated prior to reaching convergence was defined at the end of each run by plotting likelihood scores as a function of the number of generations in Microsoft (Redwood, Washington, USA) Excel 98. A Perl script that parses the MrBayes v3.0b4 log file extracting likelihood values of the cold chain in tabbed format was written to facilitate this procedure (available from R. H. Nilsson at <http://andromeda.botany.gu.se/bayesparser.zip>). Finally, a 50% majority-rule consensus tree was generated including the proportion of trees after the burn-in period to calculate posterior probability values.

Phylogenetic analyses of the ITS data set—The ITS data set was assembled including sequences of three *M. dilseae* collections and 29 additional sequences of species that were closely related to *M. dilseae* based on the results of the four-region rDNA analyses. The ITS data were analyzed in PAUP* using maximum likelihood under the GTR + Γ + I model (estimated with MODELTEST 3.06) with nucleotide frequencies estimated (A = 0.25500, C = 0.17900, G = 0.20420, T = 0.36180), a rate matrix of substitutions (A-C = 1.72800, A-G = 3.451400, A-T = 1.560000, C-G = 1.608900, C-T = 4.526200, G-T = 1.000000), proportion of invariable sites = 0.2121, and $\alpha = 1.0415$. In addition, a likelihood bootstrap analysis was performed under the same settings using 100 replicates with MAXTREES set to 1000.

RESULTS

The partial four-region data set: sequences, matrices, and tests for conflict—PCR products of *M. dilseae* were obtained from nuc-ssu (1107 base pairs [bp] product with primer combination PNS1–NS41; no product was obtained with NS19b–NS8, nuc-lsu (954 bp), and mt-lsu (498 bp) regions, whereas the amplification of a mt-ssu product failed, likely due to an insertion at one of the primer hybridization sites (Bruns et al., 1998). The closest hits in preliminary BLASTN searches (Altschul et al., 1997) using the nuc-lsu sequence of *M. dilseae* as query suggested relationships to several species in the /physalacriaceae clade as defined by Moncalvo et al. (2002). *Cylindrobasidium laeve* (Pers.) Chamuris was retrieved as best match blasting nuc-ssu and mt-lsu sequences of *M. dilseae*, followed by a number of species in different families of euagarics, which is in consequence of a more limited availability of both genes for euagarics in GenBank. We observed a base composition asymmetry toward A-T substitutions in all nuclear encoded rDNA genes of *M. dilseae*. The A-T content is slightly increased in the nuc-ssu region (2.37% mean average increase), moderately increased in the nuc-lsu region (15.51%), and extremely elevated in the ITS region (40.36%, see *Sequence characteristics and alignment of the ITS data set*) compared to other species in the /physalacriaceae clade. Individual and combined bootstrap analyses (Table 1) supported the placement of *M. dilseae* in the /physalacriaceae clade with values from 98–100%. No positive conflict greater than 72% was observed between the data partitions, and the data were therefore combined and extended with nuc-lsu sequences as described. The final alignment of the four-region rDNA data set encompassed 3566 positions after 64 ambiguous positions were excluded, including 2159 constant characters and 945 parsimony-informative characters.

TABLE 1. Alignment statistics and bootstrap intervals evaluating potential conflict between individual and combined rDNA genes.

Statistic	nuc-rDNA	mt-ssu	mt-lsu	mt-rDNA
No. taxa included	62	55	41	35
Aligned length ^a	2789	432	345	777
No. variable characters	299	74	49	131
No. informative characters	518	224	123	317
No. resolved nodes >50%	30	22	16	16
No. resolved nodes >90%	20	16	11	11
Support for the /physalacriaceae clade (%)	98	92 ^b	100	100

^a After excluding ambiguously aligned positions.

^b In the absence of a *M. dilseae* sequence.

Phylogenetic analyses of the partial four-region rDNA data set—*Inferences under parsimony*—Parsimony ratchet (PR) analyses on the partial four rDNA regions data set using six-parameter weighted parsimony resulted in 187 most parsimonious trees with a length of 13 927 steps (CI = 0.260; RI = 0.623). For comparison, the trees had a length of 8373 steps (CI = 0.260; RI = 0.612) under equally weighted parsimony. The shortest tree (Fig. 3) was found at high frequency in all 20 runs except for one, in which trees were found that were one step longer. The /physalacriaceae clade sensu Moncalvo et al. (2002) including *M. dilseae* and *P. maipoensis* was resolved as monophyletic in all trees and received 80% bootstrap support (BS). *M. dilseae* is nested within *Rhizomarasmius pyrrocephalus* (Berk.) R. H. Petersen and *Gloiocephala phormiorum* E. Horak & Desjardin and is close to *Xerula* and *Oudemansiella* spp., however, this relationship is not supported by BS > 50%. The genus *Physalacria* is monophyletic (BS = 81%) and sister to *Cylindrobasidium* (BS = 100%), although a sister relationship is weakly supported (BS = 61%). Species of *Gloiocephala* are polyphyletic and emerge in at least three different lineages. *Armillaria* spp. form a strongly supported, basal group in the /physalacriaceae clade (BS = 94). The sister group to /physalacriaceae is a clade that was newly discovered in this study; however, this relationship is not strongly supported (BS < 50%). We named this group the Cyphella clade (BS = 88%) because it includes *Cyphella digitalis* (Alb. & Schwein.) Fr., which is the type species of “Cyphellaceae.” The Cyphella clade also contains *Campanophyllum proboscideum* (Fr.) Cifuentes & R. H. Petersen and *Cheimonophyllum candidissimum* (Berk. & M. A. Curtis) Singer, two pleurotoid saprotrophs with reduced stipes.

The Nia clade (BS = 96%) includes the three remaining marine homobasidiomycetes (*N. vibrissa*, *H. villosa*, *C. mangrovei*), the major concentration of terrestrial cyphelloid fungi, and some resupinate forms (*Dendrothele* Höhn. and Litsch.). The sister group to the Nia clade is the /omphalotaceae clade (Moncalvo et al., 2002) in this study, but as in previous studies, sister relationships of the Nia clade remain ambiguous and are not strongly supported. The six-parameter weighted PR analysis was rerun applying a topological constraint (*N. vibrissa*, *H. villosa*, and *M. dilseae* are monophyletic, leaving all remaining terminals unresolved). The shortest tree (14 129 steps, CI = 0.256, RI = 0.615) was found 225 times in 12 of the 20 runs. All shortest trees were significantly worse than the unconstrained trees when compared with the K-H test ($P = 0.001$) and the S-H test ($P = 0.000$). Thus, the hypothesis of

a single origin of marine fungi in the euagarics clade was rejected.

Bayesian inferences using heterogenous models—Two independently run MCMC analyses proceeded uniformly and converged to stable likelihood scores after 1.8×10^6 generations. Twelve thousand trees of each run (scores ranging from $-\ln L$ 45 811.083 to $-\ln L$ 45 717.306) were used to estimate Bayesian posterior probabilities (BPP) after omitting 60% of the trees as the burn-in proportion. The length of the optimal tree was 14 256 steps (CI = 0.254; RI = 0.611) under the six-parameter weighing regime and 8762 steps (CI = 0.257; RI = 0.599) under equally weighted parsimony. Chains in both runs mixed frequently before approaching stationary values, suggesting that the use of a timesaving starting tree had little topologically restraining effects on the progression of the searches. Nevertheless, we observed only a single switch of the cold chain in the first run and no switching of the cold chain in the second run within their stationary phases.

Support values obtained as BPP (Fig. 3) were fairly congruent with the BS results but higher in most cases. The placement of *M. dilseae* is identical with the results of the PR analysis, although support for the clade including *M. dilseae*, *R. pyrrocephalus*, *Xerula* spp. and *Oudemansiella* spp. is weak (BPP = 0.80). The /physalacriaceae clade, the Cyphella clade, the Nia clade, and the /omphalotaceae clade all received 1.0 BPP. In addition, Bayesian analyses weakly supported (BPP = 0.85) a sister relationship of the /physalacriaceae clade, the Cyphella clade, and the Henningsomyces-Rectipilus clade A (Bodensteiner et al., 2004), the latter consists of cyphelloid forms with tubular fruiting bodies. The major topological difference comparing Bayesian trees and weighted maximum parsimony trees is the placement of the Schizophyllum clade, which is strongly supported as sister group to the Nia clade (BPP = 1.0) in Bayesian analyses, but this relationship was not resolved under parsimony.

Sequence characteristics and alignment of the ITS data set—The ITS data set was limited to species in the /physalacriaceae clade. Nineteen ITS sequences were generated including new data for *Armillaria mellea* (Vahl) P. Kumm., *Cyptotrama asprata* (Berk.) Redhead & Ginns, *M. dilseae*, *C. laeve*, *R. pyrrocephalus*, *Strobilurus trullisatus* (Murrill) Lennox and various selected species in the genera *Gloiocephala* and *Physalacria* (Appendix). Material of *Rhodotus palmatus* (Bull.) Maire, a stipitate-pileate form placed close to *Cylindrobasidium* and *Physalacria* in the four-region rDNA analyses was not available for this study. The length of ITS products ranged from 695 bp in *Physalacria maipoensis* to 913 bp in *C. asprata*. The sequence of the latter was too divergent to be aligned across all the remaining species, and *C. asprata* was consequently omitted from the ITS data set.

The ITS products of *M. dilseae* were obtained from fungal fruiting bodies using primers ITS1-F-ITS4 and from the initial stages and the later stages of using primers specific for *M. dilseae*, but not from seemingly uninfected material of *Dilsea carnosa*. The full length of ITS products was 718 bp (represented by isolate BM17/85), while *M. dilseae*-specific primers, which are nested within the ITS1-F and ITS4 range, produced products from 669 bp (BM7/87) up to 684 bp (BM16/85). All 13 *M. dilseae* ITS sequences obtained were nearly identical with the exception of strain BM7/87 lesion

number 1.2, which had five substitutions in noncoding spacer regions.

The nucleotide variation in ITS sequences of *M. dilseae* showed increased rates of both G→A and C→T transitions leading toward elevated AT mutational bias in both spacer regions, including structurally constrained regions. Transitions were also present in five positions of the 5.8S gene. The observed G-C content of *M. dilseae* ITS sequences (25.9%) was considerably lower than in closely related species, for example, 40.08–43.11% in *Gloiocephala* spp., 44.17% in *R. pyrrocephalus*, or 44.2% in *S. trullisatus*. This result is consistent with cloning experiments using two full-length *M. dilseae* ITS products that yielded only the already established copy, which was confirmed by sequencing. Preliminary studies on the secondary structure (data not shown) of ITS1 and ITS2 spacer regions of *M. dilseae*, *R. pyrrocephalus*, and *Gloiocephala* spp. using mFOLD with the default temperature settings produced similar results for all fungi included, recognizing one multibranch loop with three helices in the ITS1 region and one multibranch loop with four helices in the ITS2 region. We included *M. dilseae* sequences in the analysis of the ITS data set in accordance with structural constraints and pruned several short insertions that were present in *A. mellea* and *C. laeve* sequences. The final ITS alignment including 32 terminals consisted of 839 characters after the exclusion of 195 ambiguous positions. Of the remaining characters, 373 were constant, 99 were variable, and 367 were informative.

Phylogenetic analyses of the ITS region—The optimal tree inferred under the maximum likelihood criterion using the GTR + Γ + I model had a likelihood of -6403.1848 (Fig. 4). With weak support (BS = 56%), *M. dilseae* was nested within a clade that contains *Gloiocephala* spp., *R. pyrrocephalus*, and *Xerula* spp. pro parte with *S. trullisatus* as sister group (BS = 100%). The monophyly of *Gloiocephala* was again ambiguous; however, a sister relationship between *M. dilseae* and *G. phormiorum* was not supported, and this branch collapsed in the strict consensus of the BS analysis. In addition, *Xerula* was not monophyletic in this analysis and formed a second clade with *Oudemansiella* spp. (BS = 100%). *Physalacria* including the second marine species in the /physalacriaceae clade, *P. maipoensis*, formed a clade with *C. laeve* and *Flammulina* spp. (BS = 91%). The core of the /physalacriaceae clade excluding *Armillaria* spp., which were used for rooting purpose, received strong support (BS = 100%).

DISCUSSION

A second lineage of marine homobasidiomycetes—The higher-level, partial four-region analyses and independent analyses of individual rDNA regions suggest that *Mycaureola dilseae* represents an independent transition to marine habitat in homobasidiomycetes. Constrained analyses reject the

hypothesis that *N. vibrissa* and *M. dilseae* have been derived from a single clade. Thus, the similarities between *N. vibrissa* and *M. dilseae* (minute hemispherical fruiting bodies, statismospory, elongate spores or spore appendages) are due to convergence, presumably related to selection for the marine environment. Both *N. vibrissa* and *M. dilseae* are closely related to reduced terrestrial forms, suggesting that the presence of reduced fruiting bodies may predispose homobasidiomycetes to transitions to marine habitats.

Phylogenetic position of *M. dilseae* in the euagarics clade—The closest terrestrial relative of *M. dilseae* within the /physalacriaceae clade was not identified with confidence. The /physalacriaceae clade contains a diverse mix of reduced forms (*Gloiocephala*, *Physalacria*) as mentioned previously, as well as typical, robust agaricoid forms, including the “humungous fungus” *Armillaria* and the cultivated enokitake mushroom *Flammulina velutipes* (Curtis) Singer. If fruiting body reduction is a precursor to transitions to an aquatic habitat, then we suspect that the closest relative of *Mycaureola* is to be found among the reduced members of the /physalacriaceae clade. This is consistent with the maximum likelihood analysis of ITS data, which places *G. phormiorum* as the sister group of *Mycaureola*, albeit without bootstrap support. Furthermore, *Gloiocephala* includes one freshwater species, *G. aquatica*, that grows on submerged culms in eutrophic lakes in Argentina (Desjardin et al., 1995). Remarkably, there is another independent marine form in the /physalacriaceae clade, represented by *P. maipoensis*. Our analyses indicate that this species is not closely related to *M. dilseae* but to *Cylindrobasidium* and *Flammulina*. It has been debated, however, whether *P. maipoensis* is marine or “halotolerant” (Inderbitzin and Desjardin, 1999) because all the remaining species in the genus (approximately 32) are terrestrial and *P. maipoensis* occurs not only in intertidal zones of mangroves, but also in the adjacent forests which are not inundated. Nevertheless, the unique ecology of mangroves may have promoted multiple transitions from terrestrial to marine habitats (Hibbett and Binder, 2001).

Spore dispersal in aquatic habitats—The infection mode of *M. dilseae* is still somewhat elusive but the fungus seems very efficient infecting *Dilsea carnosus* blades. Our results from screening multiple samples of algal tissue from three different collections using *M. dilseae* specific primers confirm Porter and Farnham’s (1986) observation based on SEM microscopy that fungal mycelium is restricted within the boundary of lesions, while areas adjacent to lesions are exempt from hyphae. It is therefore unlikely that *M. dilseae* includes an endophytic step in its life cycle, living dormant within the algal tissue without producing any symptoms of an infection. The locally restricted growth pattern poses a rather challenging constraint on spore dispersal strategies in aquatic habitats. Most fungi in the /physalacriaceae clade are heterothallic (self-

Fig. 3. Phylogenetic relationships of *Mycaureola dilseae* inferred from the partial four-region data set (nuc-ssu, nuc-lsu, mt-ssu, mt-lsu) using six-parameter weighted parsimony. Shown is tree 1 of 187 (13927 steps; CI = 0.260; RI = 0.623). One hundred and one species of euagarics that are not closely related to *M. dilseae* are not shown in this figure (arrowhead). The two clades including marine fungi (the Nia clade and the /physalacriaceae clade) are projected forth by gray gradient bars, which do not contribute to branch length. Species names of marine fungi are in boldface type. Parsimony bootstrap values >55% and Bayesian posterior probabilities >0.75 are indicated along branches. The strain number is provided for published and unpublished data whenever available.

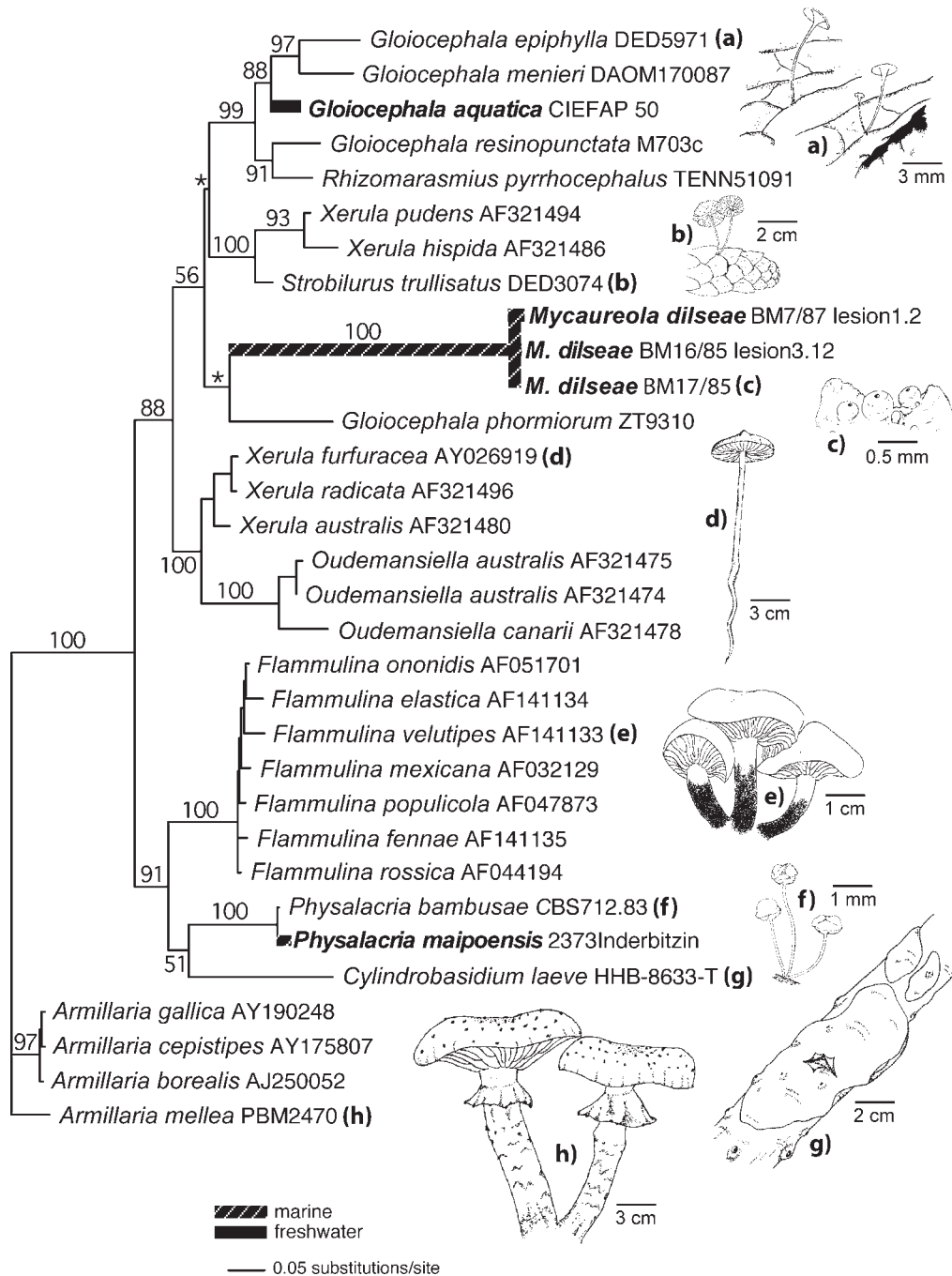


Fig. 4. Phylogenetic placement of *Mycaureola dilseae* in the /physalacriaceae clade inferred from the ITS data set using maximum likelihood under the GTR + Γ + I model ($-\ln L = 6403.1848$). ML bootstrap values $>50\%$ are indicated along supported nodes. Nodes marked with asterisks collapse in the bootstrap strict consensus tree. Shaded branches and species names written in boldface type indicate aquatic forms in the /physalacriaceae clade. The GenBank accession number is provided for published sequences, and the strain number is provided for newly generated data. The morphological diversity of fruiting body forms in the /physalacriaceae clade is illustrated with selected species: a) *Gloiocephala epiphylla*, b) *Strobilurus trullisatus*, c) *Mycaureola dilseae*, d) *Xerula furfuracea*, e) *Flammulina velutipes*, f) *Physalacria bambusae*, g) *Cylindrobasidium laeve*, and h) *Armillaria mellea*.

sterile) and have two mating genes with multiple allelic forms (Petersen et al., 1999). Producing sexual offspring requires the mating of two compatible monokarya (haploid mycelia growing from uninucleate spores) to establish a dikaryon ($n + n$) that gives rise to fruiting bodies. Under this scenario, repeated infections via additional single basidiospores have to

occur successfully in a very small area on the algal blade to guarantee the sexual reproduction of *M. dilseae*.

Conclusions—This study largely contributes to our understanding of the morphological evolution of mushroom-forming fungi. Our analyses provide strong support for a single

hypothesis of phylogenetic relationships among marine homobasidiomycetes. All marine fungi with a sexual life cycle that have been sequenced so far are placed in the euagarics clade, and they form two distinct lineages: the *Nia* clade and the /physalacriaceae clade. *Mycaureola dilseae* represents an independent adaption to the marine habitat and is the only homobasidiomycete that parasitizes a red alga. Thus, transitions from terrestrial to marine habitats were equally achieved from cyphelloid and reduced stipitate-pileate precursors.

LITERATURE CITED

- ALTSCHUL, S. F., T. L. MADDEN, A. A. SCHÄFFER, J. ZHANG, Z. ZHANG, W. MILLER, AND D. J. LIPMAN. 1997. Gapped BLAST and PSI-BLAST: a new generation of protein database search programs. *Nucleic Acids Research* 25: 3389–3402.
- BINDER, M., AND D. S. HIBBETT. 2002. Higher-level phylogenetic relationships of homobasidiomycetes (mushroom-forming fungi) inferred from four rDNA regions. *Molecular Phylogenetics and Evolution* 22: 76–90.
- BINDER, M., D. S. HIBBETT, AND H.-P. MOLITORIS. 2001. Phylogenetic relationships of the marine gasteromycete *Nia vibrissa*. *Mycologia* 93: 679–688.
- BRUNS, T. D., T. M. SZARO, M. GARDES, K. W. CULLINGS, J. J. PAN, D. L. TAYLOR, T. R. HORTON, A. M. KRETZER, M. GARBELOTTO, AND Y. LI. 1998. A sequence database for the identification of ectomycorrhizal basidiomycetes by phylogenetic analysis. *Molecular Ecology* 7: 257–272.
- BODENSTEINER, P., M. BINDER, J.-M. MONCALVO, R. AGERER, AND D. S. HIBBETT. 2004. Phylogenetic relationships of cyphelloid homobasidiomycetes. *Molecular Phylogenetics and Evolution* 33: 501–515.
- CHEMIN, E. 1921. Action d'un Champignon parasite sur *Dilsea edulis* Stackhouse. *Compte rendu hebdomadaire des Séances de l'Académie des Sciences (Paris)* 172: 614–617.
- CUNNINGHAM, C. W. 1997. Is congruence between data partitions a reliable predictor of phylogenetic accuracy? Empirical testing an iterative procedure for choosing among phylogenetic methods. *Systematic Biology* 46: 464–478.
- DE QUEIROZ, A. 1993. For consensus (sometimes). *Systematic Biology* 42: 368–372.
- DESJARDIN, D. E., L. MARTÍNEZ-PECK, AND M. RAICHENBERG. 1995. An unusual psychrophilic aquatic agaric from Argentina. *Mycologia* 87: 547–550.
- HIBBETT, D. S. 1996. Phylogenetic evidence for horizontal transmission of group I introns in the nuclear ribosomal DNA of mushroom-forming fungi. *Molecular Biology and Evolution* 13: 903–917.
- HIBBETT, D. S. 2004. Trends in morphological evolution in homobasidiomycetes inferred using maximum likelihood: a comparison of binary and multistate approaches. *Systematic Biology* 53: 891–915.
- HIBBETT, D. S., AND M. BINDER. 2001. Evolution of marine mushrooms. *Biological Bulletin* 201: 319–322.
- HIBBETT, D. S., AND M. BINDER. 2002. Evolution of complex fruiting-body morphologies in homobasidiomycetes. *Proceedings of the Royal Society London, B, Biological Sciences* 269: 1963–1969.
- HIBBETT, D. S., E. M. PINE, E. LANGER, G. LANGER, AND M. J. DONOGHUE. 1997. Evolution of gilled mushrooms and puffballs inferred from ribosomal DNA sequences. *Proceedings of the National Academy of Sciences, USA* 94: 12002–12006.
- HYDE, K. D., V. V. SARMA, AND E. B. G. JONES. 2000. Morphology and taxonomy of higher marine fungi. In K. D. Hyde and S. B. Pointing [eds.], *Marine mycology: a practical approach*, 172–204. Fungal Diversity Research Series 1, Fungal Diversity Press, Hong Kong, China.
- INDERBITZIN, P., AND D. E. DESJARDIN. 1999. A new halotolerant species of *Physalacria* from Hong Kong. *Mycologia* 91: 666–668.
- KIRK, P. M., P. F. CANNON, J. C. DAVID, AND J. A. STALPERS. 2001. Ainsworth and Bisby's dictionary of the Fungi, 9th ed. CAB International, Wallingford, Oxon, UK.
- KISHINO, H., AND M. HASEGAWA. 1989. Evaluation of the maximum likelihood estimate of the evolutionary tree topologies from DNA sequence data, and the branching order in Hominoidea. *Journal of Molecular Evolution* 29: 170–179.
- KOHLMEYER, J., AND E. KOHLMEYER. 1979. *Marine mycology: the higher Fungi*. Academic Press, New York, New York, USA.
- LEE, S. B., AND J. W. TAYLOR. 1990. Isolation of DNA from fungal mycelia and single cells. In M. A. Innis, D. H. Gelfand, J. J. Sninsky, and T. J. White [eds.], *PCR protocols: a guide to methods and applications*, 282–287. Academic Press, San Diego, California, USA.
- MADDISON, D. R., AND W. P. MADDISON. 2000. *MacClade 4: analysis of phylogeny and character evolution*. Sinauer, Sunderland, Massachusetts, USA.
- MAIRE, R., AND E. CHEMIN. 1922. Un nouveau Pyrénomycète marin. *Compte rendu hebdomadaire des Séances de l'Académie des Sciences (Paris)* 175: 319–321.
- MATHENY, P. B. 2004. Improving phylogenetic inference of mushrooms with RPB1 and RPB2 nucleotide sequences (*Inocybe*; Agaricales). *Molecular Phylogenetics and Evolution* 35: 1–20.
- MONCALVO, J.-M., F. M. LUTZONI, S. A. REHNER, J. JOHNSON, AND R. VILGALYS. 2000. Phylogenetic relationships of agaric fungi based on nuclear large subunit ribosomal DNA sequences. *Systematic Biology* 49: 278–305.
- MONCALVO, J.-M., R. VILGALYS, S. A. REDHEAD, J. E. JOHNSON, T. Y. JAMES, M. C. AIME, V. HOFSTETTER, S. J. W. VERDUIN, E. LARSSON, T. J. BARONI, R. G. THORN, S. JACOBSSON, H. CLÉMENÇON, AND MILLER K JR. 2002. One hundred and seventeen clades of euagarics. *Molecular Phylogenetics and Evolution* 23: 357–400.
- MOORE, R. T., AND S. P. MEYERS. 1959. Thalassiomycetes. I. Principles of delimitation of the marine mycota with description of a new aquatically adapted deuteromycete genus. *Mycologia* 88: 871–876.
- NIXON, K. C. 1999. The parsimony ratchet, a new method for rapid parsimony analysis. *Cladistics* 15: 407–414.
- PETERSEN, R. H., K. W. HUGHES, S. A. REDHEAD, N. PSURTSEVA, AND A. S. METHVEN. 1999. Mating systems in the Xerulaceae (Agaricales, Basidiomycotina): *Flammulina*. *Mycoscience* 40: 411–426.
- PORTER, D., AND W. F. FARNHAM. 1986. *Mycaureola dilseae*, a marine basidiomycete parasite of the red alga, *Dilsea carnosa*. *Transactions of the British Mycological Society* 87: 575–582.
- POSADA, D., AND K. A. CRANDALL. 2001. Selecting the best-fit model of nucleotide substitution. *Systematic Biology* 50: 580–601.
- RONQUIST, F., AND J. P. HUELSENBECK. 2003. MrBayes 3: Bayesian phylogenetic inference under mixed models. *Bioinformatics* 19: 1572–1574.
- SHIMODAIRA, H., AND M. HASEGAWA. 1999. Multiple comparison of log-likelihoods with applications to phylogenetic inference. *Molecular Biology and Evolution* 16: 1114–1116.
- SIKES, D. S., AND P. O. LEWIS. 2001. Beta software, version 1. PAUPRat: PAUP* implementation of the parsimony ratchet. Distributed by the authors, Department of Ecology and Evolutionary Biology, University of Connecticut, Storrs, Connecticut, USA. Available at website <http://viceroy.eeb.uconn.edu/paupratweb/pauprat.htm>.
- STANGER-HALL, K., AND C. W. CUNNINGHAM. 1998. Support for a monophyletic Lemuriformes: overcoming incongruence between data partitions. *Molecular Biology and Evolution* 15: 1572–1577.
- SWOFFORD, D. L. 2002. PAUP*: phylogenetic analysis using parsimony (*and other methods), version 4.0b10. Sinauer, Sunderland, Massachusetts, USA.
- THOMPSON, J. D., T. J. GIBSON, F. PLEWNIAK, F. JEANMOUGIN, AND D. G. HIGGINS. 1997. The ClustalX windows interface: flexible strategies for multiple sequence alignment aided by quality analysis tools. *Nucleic Acids Research* 25: 4876–4882.
- VILGALYS, R., AND M. HESTER. 1990. Rapid genetic identification and mapping of enzymatically amplified ribosomal DNA from several *Cryptococcus* species. *Journal of Bacteriology* 172: 4238–4246.
- WHITE, T. J., T. D. BRUNS, S. LEE, AND J. TAYLOR. 1990. Amplification and direct sequencing of fungal ribosomal RNA genes for phylogenetics.

- In M. A. Innis, D. H. Gelfand, J. J. Sninsky, and T. J. White [eds.], PCR protocols: a guide to methods and applications, 315–322. Academic Press, San Diego, California, USA.
- WILLIAMS, P. L., AND W. M. FITCH. 1990. Phylogeny determination using the dynamically weighted parsimony method. *Methods in Enzymology* 183: 615–626.
- YANG, Z. 1994. Estimating the pattern of nucleotide substitution. *Journal of Molecular Evolution* 39: 105–111.
- ZUKER, M., D. H. MATHEWS, AND D. H. TURNER. 1999. Algorithms and thermodynamics for rna secondary structure prediction. In J. Barciszewski and B. F. C. Clark [eds.], A practical guide in RNA biochemistry and biotechnology, 11–43. NATO ASI Series, Kluwer, Dordrecht, Netherlands.

APPENDIX. Taxa, isolate numbers, geographical origin, and GenBank accession numbers. GenBank accession numbers for sequences generated in this study are in boldface; other sequences are from our earlier studies.

Taxon; *Voucher* (Herbarium code); *Locality*; *ITS*; *nuc-lsu*; *nuc-ssu*; *mt-lsu*; *mt-ssu*.

- Armillaria mellea* (Vahl) P. Kumm.; *PBM 2470*, *AFTOL-ID 449* (Clark); USA; **AY789081**; **AY700194**; **AY787217**; —; —.
- Auriculariopsis ampla* (Lév.) Maire; *NH-1803* (GB); Spain; **DQ097353**; AY293169; —; AY293251; AY293222.
- Cylindrobasidium laeve* (Pers.) Chamuris; *HHB-8633-T* (CFMR); USA; **DQ097354**; AF518611; AF518576; AF518705; AY293224.
- Cyptotrama asprata* (Berk.) Redhead & Ginns; *DED6391*, *AFTOL-ID 1342* (SFSU); USA; **DQ097355**; —; —; —.
- Flagelloscypha minutissima* (Burt) Donk; 823.88 (CBS); Germany; AY571040; AY571006; —; **DQ097371**; —.
- Flagelloscypha* sp.; *Horak 9544*; (ZT); USA; AY571041; AY571007; —; **DQ097375**; —.
- Gloiocephala aquatica* Desjardin, Mart.-Peck & Rajchenb.; *CIEFAP50*, *AFTOL-ID 517* (BAFC); Argentina; **DQ097356**; **DQ097343**; **AY705968**; **DQ097372**; **DQ097379**.
- Gloiocephala epiphylla* Masee; *DED5971* (SFSU); USA; **DQ097357**; **DQ097344**; —; —; —.
- Gloiocephala menieri* (Boud.) Singer; *170087* (DAOM); Canada; **DQ097358**; **DQ097345**; —; —; **DQ097380**.
- Gloiocephala phormiorum* E. Horak & Desjardin; *Horak 9310* (ZT); New Zealand; **DQ097359**; **DQ097346**; —; —; —.
- Gloiocephala resinopunctata* Manim. & K.A. Thomas; *M703c* (SFSU); India; **DQ097360**; —; —; —; —.
- Gloiocephala* sp.; *DED7649* (SFSU); Malaysia; **DQ097361**; —; —; —; —.
- Henningsomyces* sp.; *FP-105017-Sp.* (CFMR); USA; AY571047; AY571010; **DQ097341**; —; —.
- Lachnella villosa* (Pers.) Gillet; *609.87*, *AFTOL-ID 525* (CBS), Netherlands; **DQ097362**; **DQ097347**; **AY705959**; **DQ097373**; **DQ097381**.
- Limnoperdon incarnatum* G.A. Escobar; *30398* (IFO); Japan; **DQ097363**; AF426958; AF426952; AF426969; AF426964.
- Mycaureola dilseae* (Maire & Chemin) emend. Porter & Farnham; *17/85* (BM); Great Britain; **DQ097364**; **DQ097348**; **DQ097342**; **DQ097374**; —.
- Mycaureola dilseae* (Maire & Chemin) emend. Porter & Farnham; *16/85* (BM); Great Britain; **DQ097366**; —; —; —; —.
- Mycaureola dilseae* (Maire & Chemin) emend. Porter & Farnham; *7/87* (BM); Great Britain; **DQ097365**; —; —; —; —.
- Physalacria bambusae* Höhn.; 712.83, *AFTOL-ID 515* (CBS); Japan; **DQ097367**; **DQ097349**; AY705953; **DQ097376**; **DQ097382**.
- Physalacria maipoensis* Inderb. & Desjardin; *2373 Inderbitzin* (—); Thailand; **DQ097368**; AF426959; AF426953; AF426970; AF426965.
- Plicaturopsis crispa* (Pers.) D.A. Reid; *MB-1301* (Clark); USA; —; **DQ097350**; —; —; —.
- Rhizomarasmius pyrrocephalus* (Berk.) R.H. Petersen; *51091* (TENN), USA; **DQ097369**; **DQ097351**; —; —; —.
- Schizophyllum fasciatum* Pat.; *267.60* (CBS); USA; —; —; —; **DQ097377**; —.
- Schizophyllum radiatum* (Sw.) Fr.; *301.32*, *AFTOL-ID 516* (CBS); Panama; **AY571060**; AY571023; **AY705952**; **DQ097378**; **DQ097383**.
- Strobilurus trullisatus* (Murrill) Lennox; *DED3074* (SFSU); USA; **DQ097370**; **DQ097352**; —; —; —.